Incorporation of the effects of salinity, nitrogen stress, and shading into an algae growth model and evaluation in the ARID raceway

Song Gao, Peter Waller, George Khawan, Said Attalah, Michael Huesemann, Kimberly Ogden

Abstract

The Huesemann Algae Biomass Growth (HABG) model predicts microalgae biomass growth in outdoor raceways as a function of water temperature and incident light intensity. The model over-predicted growth in several Regional Algal Feedstock Testbed (RAFT) experiments. Inspection of the culture conditions suggested that salinity stress, nutrient limitation, and shading reduced growth, which were not included in the original model. Laboratory experiments were carried out to measure growth response of *S. obliquus* to high salinity and limited nitrogen. In addition, the shading effect was estimated based on raceway geometry, solar angle, albedo and measured light intensity data. In this study, the improvement of model performance is presented step by step as each growth limiting factor is incorporated into the model. The new salinity, shanding, and nutrient stress factors remove most of the over-prediction of the original model. Comparison of the model with observed data indicated that ignoring the lag phase also resulted in overprediction. Delaying the start of the simulation until the end of the lag phase and inclusion of stress factors lowered model inaccuracy from 90% over-prediction to within ±10% in six out of seven batches.

Key Words: Huesemann algae biomass growth model, ARID raceway, salinity, nitrogen, shading

1. Introduction

Many algae growth models have input parameters such as light, temperature, and nutrient concentration (Bannister, 1979; Cornet and Dussap, 2009; Quinn et al., 2011; Yuan et al., 2014). Some models are designed to incorporate reduced growth rates under conditions such as low nitrogen concentration or limiting light intensity (Goldman and Hole, 1979; James and Boriah, 2010; Packer et al., 2011). The Huesemann Algae Biomass Growth (HABG) model (Huesemann et al., 2016), which requires light and temperature as input variables. Growth rate coefficients were measured over a range of light intensities and temperature in the laboratory experiments. The model was thus able to predict the biomass growth rate as a function of temperature and light in algae raceways (Huesemann et al. 2016). Because the model assumes that all conditions other than temperature and light are optimal, it must be adjusted in cases when other parameters are not optimal.

Some high salinity adapted algal strains such as *Dunaliella* can be maintained as monoculture in open raceway ponds with high salinity (Rao et al., 2012). Increasing culture salinity has been proposed as a method to control contamination by organisms that have low tolerance for salinity. However, high salinity inhibits the growth of many algal species, particularly freshwater algal strains (Kaewkannetra et al., 2012; Mohammed and Shafea, 1992; Rao et al., 2007). Kaewkannetra et al. (2012) found that salinity of 0.05M (1.42 g/L) sodium chloride stressed *S. obliquus* and caused a significant decrease in growth rate.

Nitrogen is one of the major algae nutrient requirements, and nitrogen status in the culture has a strong impact on biomass productivity (Converti et al., 2009; Hsieh and Wu, 2009; Wijffels and Barbosa, 2010). It is also one of the major costs in microalgal biomass production (Rogers et al., 2014). In the RAFT (Regional Algal Feedstock Testbed) project, researchers attempted to reduce nitrogen fertilization rate in

order to reduce cost and environmental impact, but in the process caused intermittent nitrogen stress in the culture. Thus, to realistically simulate algal growth in these experiments, it was necessary to quantify the effect of nitrogen stress on algal growth.

Algal growth rate is highly sensitive to light intensity (Difusa et al., 2015; Sorokin and Krauss, 1958; Yoshimura et al., 2013). Although not commonly an issue in large outdoor raceways, many experimental raceways have significantly reduced light intensity due to shading from walls. The HABG assumes unshaded conditions and was constructed with data obtained from unshaded indoor laboratory cultures. The model must be adjusted for shading in order to obtain accurate prediction of algae growth in shaded experimental raceways.

The goal of the current research was to introduce stress effects such as salinity, nitrogen limitation, and shading to the HABG model and to simulate *S. obliquus* growth rate in outdoor raceway experiments with measured water temperature and light intensity data in the ARID (Algae Raceway Integrate Design) raceway (Waller et al., 2012). The simulations were evaluated against experimental data to evaluate the modification.

2. **Materials and Methods**

2.1 Outdoor culture system

The ARID open pond raceway, was utilized in the current study. It is located at Campbell Avenue Agriculture Center, the University of Arizona, Tucson, AZ (32° 16' 49" N / 110° 56' 45" W). This version of the ARID raceway is 16 m in length and 5 m in width, consisting of 22 shallow channels and one deep canal (Fig. 1). Channels were separated by plastic baffles. The baffles are 15 cm in height and the channels are 45 cm in width. The canal shape is a 1.5 m deep inverted rectangular frustum. The top area is 5 m by 3.6 m rectangle, and the bottom area is 2 m by 0.6 m rectangle. The side slope is 45°.

During daytime, water flowed through a labyrinth of east-west channels by gravity from north to south. Culture was circulated from the last lower channel and the canal to the upper channel using pumps. driven by solar energy. Daytime culture depth was maintained at 0.1 m in the channels, and 0.3 m in the canal. During night, the culture drains entirely into the canal. Thermal insulation in the canal protects algae from adverse environmental conditions during night, such as low temperature. When the sun rises in the morning, the pump starts circulating the water through the raceway.

Two experiments, RAFT06 and RAFT07, were conducted from 7th January to 2nd March and from 16th March to 30th April, 2015 with *S. obliquus,* respectively. The pH was controlled by on-demand periodic CO_2 injection and was maintained at 8.0. Nutrients were added to give an initial concentration of 50 mg urea/L, 10 mg ammonium diphosphate/L, and 12 mg magnesium sulfate/L. Other micronutrients were added according to the BG-11 nutrient recipe (Rippka et al., 1979). The standard protocol was to fertilize with the same nutrient constituents with every 0.25 AFDW (ash free dry weight) increment. In an attempt to control pests, initial salinity was increased to the range of 5 g/L by adding NaCl. Electric conductivity (EC) was used to measure salinity, and a calibration curve was obtained prior to the experiment to determine the relationship between salinity and EC reading. In this study, salinity was expressed as equivalent to g-NaCl/L. Measured EC was averaged over one-day increments in the model.

In this experiment, the standard protocol was to harvest when biomass concentration reached 0.8 g/L ash free dry weight (AFDW). Three harvests took place (DOY (day of year) 92, DOY 100 and DOY 112), with approximately half of the biomass and two thirds of culture media removed from the raceway each

time. After each harvest, the raceway was replenished with water to the original volume, and nutrients were added. In the model, initial biomass concentration for simulations was reset to observed concentration after harvest dilution.

Fig. 1. The ARID (Algae Raceway Integrate Design) raceway used in this experiment.

2.2 Data collection and biomass concentration measurement

Temperature, pH and electric conductivity were recorded with a Campbell Scientific CR3000 datalogger. Readings from sensors were averaged every 5 seconds and recorded every 10 minutes. Optical density (OD) was measured manually using a spectrophotometer (Spectronic Genesys^{TM} 5, Thermo Fisher Scientific Inc. Waltham, MA, USA) at 750 nm, at 9:00 am after refilling the pond with water to the initial volume. Biomass concentration was then converted from OD to AFDW. AFDW was measured by filtering, drying at 75 ℃ overnight and ashing the sample at 550 ℃ for 4 hours. Correlation of OD and AFDW was found to be linear, following Equation (1).

$$AFDW = 0.5023 * OD_{750} \ (R^2 = 0.98) \quad (1)$$

Solar radiation was obtained from Arizona Meteorological Network (AZMET), measured with LI-COR LI-200 silicon cell pyranometer. Solar radiation data (MJ/m^2/hr) reported by the weather station was converted to Photosynthetically Active Radiation (PAR) (μmole/m^2-s). The following equation was used for the conversion (Thimijan and Heins, 1983):

$$\left(\frac{MJ}{hr\ m^2}\right) = 581.4\ \frac{\mu mole}{s\ m^2}(PAR) \quad (2)$$

2.3 Theoretical development of stress factors

Edmundson et al. (, n.d.)measured growth rate of *S. obliquus* as a function of light intensity and water temperature (Equation 3).

$$\mu = \mu(T, I) \quad (3)$$

Where, T is water temperature (°C), I is light intensity (μmol/m^2-s)

Growth rate reduction caused by salinity stress, nitrogen limitation, and shading effect were represented by three factors in the model, namely, salinity factor, nitrogen factor and shading factor. Each factor, ranging from 0 to 1, is a multiplier in the growth rate calculation equation (Equation 4). The factor is 0 if the corresponding stress is severe enough to prevent any growth, between 0 and 1 if the stress lowers growth rate but does not completely stop growth, and 1 if the there is no reduction due to the stress factor. This section describes how stress factors were determined as a function of the nitrogen, salinity, or shading status.

$$\mu = F_S F_N \mu(T, R_Z I) \quad (4)$$

Where F_S is salinity factor, F_N is nitrogen factor, R_Z is shading factor

2.3.1 Measurement of the specific growth rate as a function of salinity and salinity factor

The specific growth rate of *S. obliquus* as a function of salinity was determined at room temperature in shaker flask cultures containing BG-11 media amended with different concentrations of Instant OceanTM. The incident light intensity was above 400 μmol/m^2-s and the cultures were kept sufficiently thin to ensure that all cells received above saturating light intensity (>200 μmol/m^2-s) and thus were growing exponentially at their maximum specific growth rate. The cultures were sparged with CO_2-enriched air to maintain an equilibrium pH of 7.5. The specific growth rate, μ_s, at different salinities was determined from the slope of ln(OD_{750}) versus time (Van Wagenen et al., 2014).

The maximum specific growth rate, $\mu_{max\text{-}s}$, is expected below the salinity threshold. Growth rate μ_S, decreases linearly with increasing salinity up to the point that growth is zero. The growth rate fraction ($\mu_s/\mu_{max\text{-}s}$) is the salinity factor (F_s).

2.3.2 Measurement of specific growth rate as a function of nitrogen availability and nitrogen factor
In previous study (Gao et al. n.d.), *S. obliquus* was cultured in a flat-panel photobioreactor in the laboratory at room temperature, provided with CO_2-enriched air, and light intensity 360 μmol/m^2-s (measured by LI-COR 190 R quantum sensor, LI-COR, Inc., Lincoln, Nebraska) . Cellular nitrogen content was used as a measure of nitrogen stress intensity. The alga was first cultured in nitrogen-replete medium (BG-11), where maximum cellular nitrogen content was obtained. Then nitrogen-depleted BG-11 medium was used. The culture experienced 12h light:12 h dark cycles. At the beginning of each light period, the culture was diluted to the same biomass concentration, approximately 0.32 g-dry mass/L, in order to normalize light attenuation effect on growth. Specific growth rate (μ_N) as a function of cellular nitrogen content was determined from biomass accumulation during the light period (Van Wagenen et al., 2014). The experiment continued until no growth was observed during the light period. Maximum growth rate ($\mu_{max\text{-}N}$) was obtained above a threshold cellular nitrogen content, and minimum cellular nitrogen content was measured when there was no growth ($\mu_N \leq 0$).. In the study, we introduced the concept of nitrogen availability (N_A), the ratio of total added nitrogen in fertilizer to accumulated biomass, as a measure of nitrogen stress. Total added nitrogen includes both intracellular nitrogen and extracellular

nitrogen, but it is assumed that the cell can consume all the available nitrogensuch that nitrogen absorbed in the cell has the same utility as nitrogen in the culture media, which can be absorbed at a later time.

The nitrogen factor, F_N, is the fraction of growth rate at low N_A to maximum growth rate above threshhold N_A ($\mu_N/\mu_{max\text{-}N}$). We obtained the relationship between N_A and F_N from the laboratory experiments and regresssion,. In the outdoor raceway experiments, total available nitrogen was the amount of applied nitrogen fertilizer. At each harvest, we assumed that the fraction of nitrogen removal was the same as the fraction of culture volume harvested. The remaining nitrogen plus added fertilizer wasthe initial N_A for the next culture batch.

2.3.3 Shading effect estimation

In outdoor cultivation systems, shading can significantly reduce the average light to the system. The ARID raceway version used in this study was a set of rectangular channels separated by baffles oriented in the East-West direction (Fig. 1). Shade on the north side of the board, especially in winter when solar angle is low, reduces average light to the culture. A solar path model was incorporated into the model to calculate solar angles for calculating shading change throughout the day.

To estimate the reduced incident light due to shading, two factors were considered, the area covered by shade and light intensity in the shade. Part of the incident light is reflected at the surface (albedo) and the rest enters the water at the refracted angle. Light reflection (1 – albedo) was calculated with the Fresnel equations. Fig. 2(a) shows the light beam at the edge of the shaded area. The zenith angle (θ_1) and azimuth angle (A) (from North, clockwise) were calculated at each time step. The refractive angle (θ_2) was calculated with Snell's Law. The refractive index of algae culture was measured manually with a refractometer (RF20, Extech), and was the same as that of water. Shade width (w) from the board to the edge of the shade at depth (z) was calculated with Equations 5 and 6.

$$w_z = -(H - D)\tan(\theta_1)\cos(A) - z\cot(\theta_2)\cos(A) \quad (5)$$

$$\theta_2 = \sin^{-1}(n_1 \sin\theta_1 / n_2) \quad (6)$$

where

w_z = shade width (board to edge of shade) at depth z (m)
H = board height (m)
D = culture depth (m)
θ_1 = zenith angle
θ_2 = refractive angle
A = azimuth angle (from North, clockwise)
z = depth (m)
n_1 = refractive index of air
n_2 = refractive index of water

Light intensity in shaded regions is not zero but is a fraction of the unblocked incident light, which we call the light ratio. We measured light intensity, I_{zx}, as a function of depth z and distance x from the board using a LI-250A light meter and LI-COR LI-190R quantum sensor facing vertically up (Fig. 2b). Meanwhile, light intensity at the same depth within the unshaded area was measured and denoted as I_{z0}. The light ratio at this point is expressed by Equation 7:

$$r_{zx} = I_{zx} / I_{z0} \quad (7)$$

where

I_{zx} = light intensity at point at distance x and depth z (μmol/m^2-s)
I_{z0} = light intensity in unshaded area at depth z (μmol/m^2-s)

For the entire layer at depth z, cumulative light received within the shaded area is calculated by Equation 8 and total light received within the unshaded area is calculated by Equation 9. Total light received by layer z is the sum of these two values and represented by I_z as shown by Equation 10. Due to high flow rate and mixing, we averaged sun light exposure in shaded and unshaded areas at each depth. Therefore, I_z in Equation 10 is the average light received in shaded and unshaded areas by the culture at depth z. This is an important assumption and the results are sensitive to this assumption. The other alternative is to calculate the growth rate separately in shaded and unshaded areas. The original HABG model doesn't include the shading effect, and calculates the total light at each depth as $I_{z0}L$.

$$I_{z-shaded} = \int_0^{w_z} I_{z0} r_{zx} d_x \tag{8}$$

$$I_{z-unshaded} = I_{z0}(L - w_z) \tag{9}$$

$$I_z = \int_0^{w_z} I_{z0} r_{zx} d_x + I_{z0}(L - w) \tag{10}$$

where

I_z = light received by layer z
I_{z0} = light intensity within unshaded area at depth z
L = channel width (m)
r_{zx} = light ratio of point at distance x, depth z
w_z = shade width at depth z (m)

$$R_Z = \frac{\int_0^{w_z} I_0 r_{zx} d_x + I_{z0}(L-w)}{I_{z0}L} \tag{11}$$

Dividing Equation 10 by $I_{z0}L$ calculates the fraction of light with shading over the light without considering shading. This is expressed by Equation 11 and yields the shading factor, R_z, at each depth. The product of shading factor and Beer-Lambert light intensity at each layer is the average light intensity at that layer. The geometry of the canal is slightly more complicated than the channels since the canal has sloping sides, but we accounted for the decreasing area with depth and calculated light intensity with the same integration method.

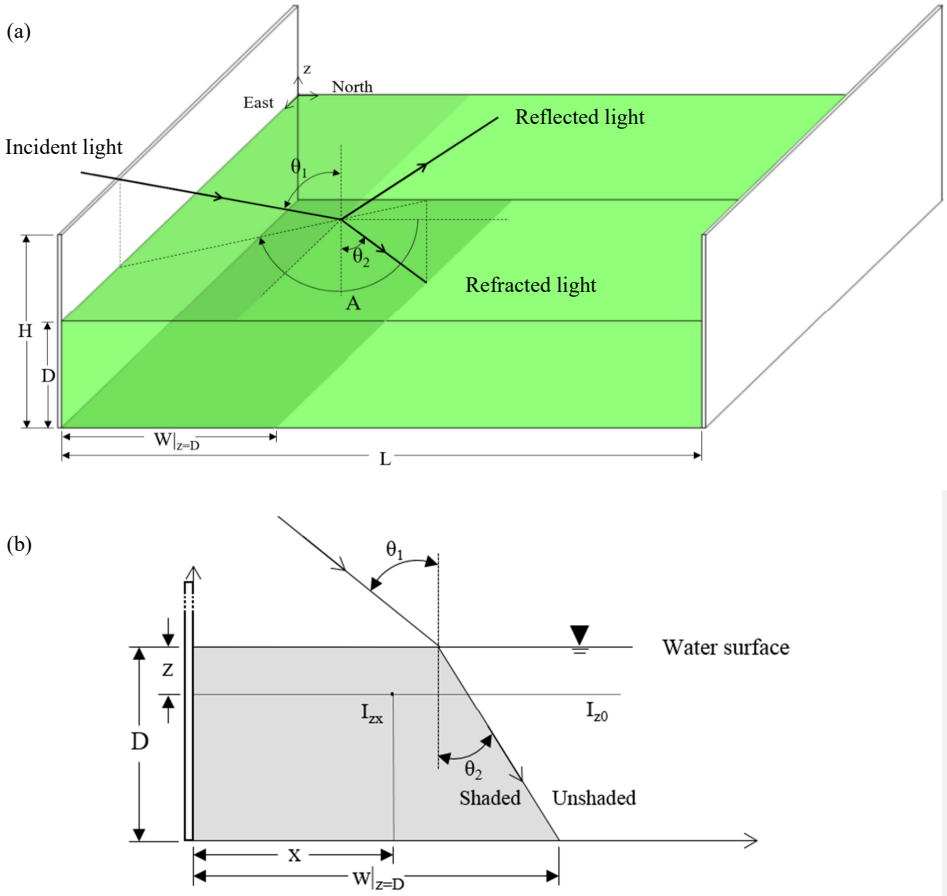

Fig. 2. (a) Dark area represents shaded area; L is channel width; w is shade length, *H* is board height; *D* is culture depth; θ_1 is zenith angle; θ_2 is refractive angle; *A* is azimuth angle (from north, clockwise) (b) Side view of raceway channel. I_{zx} is light intensity at depth *z* and distance *x*; I_{z0} is light intensity in unshaded area at depth *z*.

2.4 Simulation parameters and other assumptions

The simulation time steps were set to be the same as the datalogger recording frequency (10 mins). Due to low residence time, we assumed that temperature and salinity were uniformly distributed in the raceway. Growth was calculated in 100 vertical layers in both the channel culture and canal culture. Biomass

concentration was averaged at each time step by numerically combining the volumes of the channel culture and canal culture.

Commented [高嵩1]: Does this mean weighted average?

The effect of salinity and nitrogen on dark respiration during day and night has not been quantified in experiments. In this study, we assumed that night dark respiration rate was not affected by salinity or nitrogen stress factors. However, daytime dark respiration was adjusted by the salinity and nitrogen factors because it was part of the total culture growth rate that was adjusted during the day. Further research is required for verifying this assumption.

Although the setpoint of pH in the raceway experiments was 8.0, fluctuation occurred. The average pH was approximately 7.8 throughout the experiments. The difference from the pH at which the growth coefficients in the HABG were determined in laboratory experiments (7.5) was small, thus we assumed the growth coefficients were applicable to the raceway experiments.

2.5 Comparison of the model with experimental data

Model performance can be evaluated by comparing observed growth and predicted growth. We evaluated the root mean square error (RMSE) between simulated and experimental biomass concentration. To quantify over-prediction, we used the bias factor (BF), a concept proposed by Ross (1996), modified by Baranyi et al. (Baranyi et al., 1999) and used for microbial growth model evaluation (López et al., 2004; te Giffel and Zwietering, 1999). Perfect prediction yields a BF value of 1. A BF value greater than 1 represents over-prediction, and vice-versa.

3. Results and discussion

This section successively incorporates salinity, nitrogen and shading factors into the HABG model and compares the simulations to experimental data from the RAFT 07 ARID experiment. The final equation for growth rate calculation is shown by Equation 4.

$$\mu = F_S F_N \mu(T, R_Z I)$$

Finally, we compare the model with all factors to data collected in the RAFT 06 experiment, which was the only other *Scenedesmus* experiment conducted in the configuration of the ARID raceway described in this paper.

3.1 Original model ($\mu = \mu(T, I)$)

This section compares the original growth model to observed data from RAFT 07. Four consecutive batches were separated by three harvests (Fig. 3). Half of the media was harvested each time, and water replenishment following each harvest resulted in approximately half of the biomass as the starting concentration. The saw-tooth shaped curve in the simulation line was caused by biomass accumulation during daytime due to photosynthesis, and biomass loss during night due to dark respiration. The comparison of observed data and the simulation showed significant over-prediction with the original HABG model. The RMSE was 0.62, and 1.90 BF means that over-prediction averaged 90% for the four successive batch culture runs.

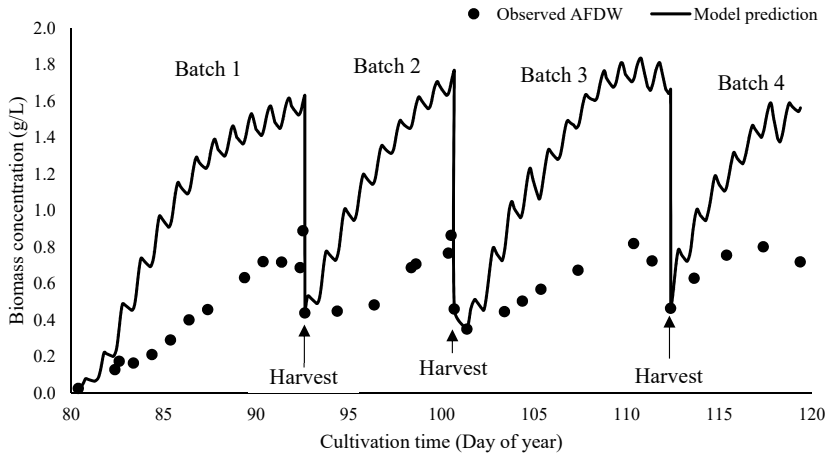

Fig. 3. Observed (●) and predicted (—) biomass concentration over time. Three harvests divided the experiment into 4 successive batch culture runs Approximately half of the biomass was removed in each harvest. Initial biomass concentration for growth simulation in each was set to the measured biomass concentration. $RMSE_1 = 0.62$, $BF_1 = 1.90$

3.2 Incorporation of salinity factor ($\mu = F_S\mu(T, I)$)

In laboratory experiments, growth response of *S. obliquus* to salinity was quantified within the salinity range of 0 to 40 g/L (Fig. 4). The curve can be divided into three sections (Equation 11). Between salinity 0 and 1 g/L, there was no growth rate reduction, thus F_S is 1. From 1 g/L to 30 g/L, specific growth rate decreased linearily with increasing salinity. F_s was obtained by linear interpolation within this range. Salinity greater than 30 g/L prevented any growth thus F_s is 0.

$$F_S = \begin{cases} 1 & (S \leq 1) \\ -0.035S + 1.2045 & (1 < S < 30) \\ 0 & (S \geq 30) \end{cases} \quad (11)$$

where S = salinity (g/L).

Salinity decreased from 3 to 4 g/L in the first two batches to 1 to 2 g/L in the latter batches (Fig. 5). Consequently, the F_S was lower (higher salinity stress) in early batches than in latter batches (Fig. 6). After adjustment for salinity effect, average over-prediction was reduced from 90% to 57% (BF = 1.57).

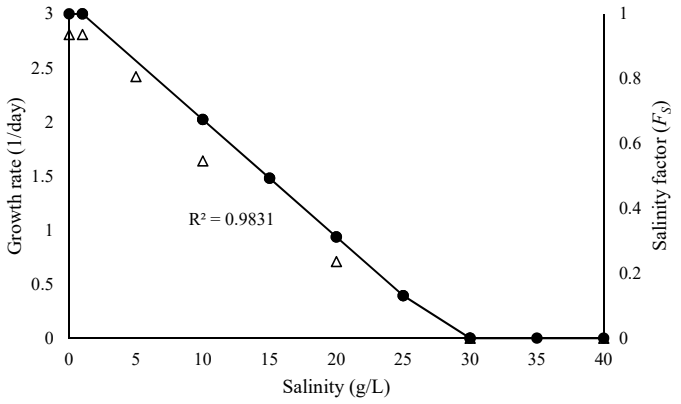

Fig. 4. Specific growth rate (△) and salinity factor (●, μ_s/μ_{max}) as a function of salinity (equivalent to g-NaCl/L) for *S. obliquus* in laboratory culture

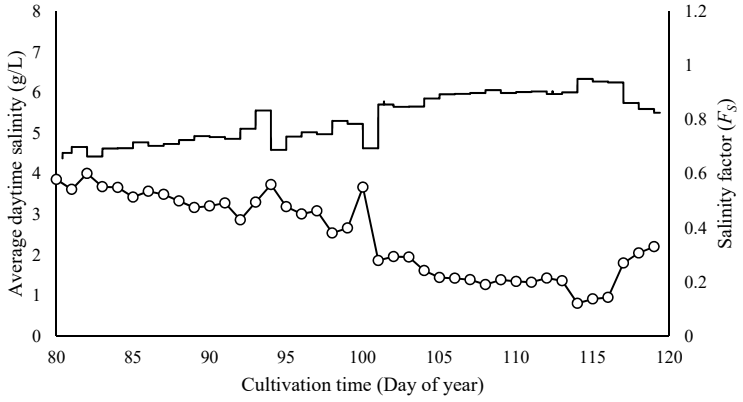

Fig. 5. Average daytime salinity (○) and corresponding salinity factor F_S (—) during RAFT07 ARID raceway experiment

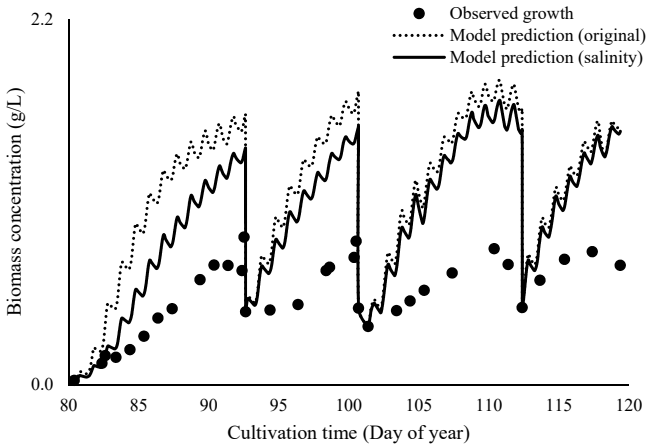

Fig. 6. Measured biomass concentration (●), original model (dashed line) and model with salinity adjustment (solid line, $RMSE_2 = 0.47$, $BF_2 = 1.57$).

3.3. Incorporation of nitrogen factor ($\mu = F_S F_N \mu(T, I)$)

Under nutrient limited conditions, the nitrogen factor can be calculated with the Droop (1968) equation. With the assumptions of full consumption of available nitrogen, we replaced Droops cell quota (Q) with nitrogen availability (N_A): the total available nitrogen in the algae culture (g/L) divided by total cell biomass in the culture.

$$\mu_N = \mu'_m - \left(k_q \mu'_m\right)\frac{1}{Q} = \mu'_m - \left(k_{NA} \mu'_m\right)\frac{1}{N_A} \tag{12}$$

Where, N_A is nitrogen availability (g/g); μ_m' is growth rate at infinite N_A; k_{NA} is the minimum N_A at zero growth rate

With measured specific growth rates and their corresponding N_A, model parameters were obtained by linear regression ($\mu_m' = 1.27$, $k_q = 0.02$). Nitrogen factor (F_N) was the fraction of growth rate at a certain N_A to the maximum growth rate observed in the experiments ($\mu_N/\mu_{max\text{-}N}$). Therefore, F_N was calculated by dividing Equation 12 with $\mu_{max\text{-}N}$ (Equation 13). Equation 13 is plotted against experiment data and is shown in Fig. 7.

$$F_N = \frac{\mu_N}{\mu_{max-N}} = \frac{\mu'_m - \left(k_{NA}\mu'_m\right)\frac{1}{N_A}}{\mu_{max-N}} = 1.33(1 - 0.022/N_A) \tag{13}$$

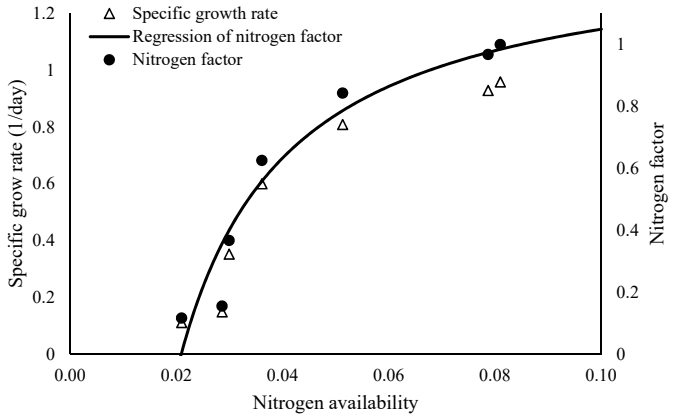

Fig. 7. Specific growth rate (μ_N, △) and nitrogen factor ($\mu_N/\mu_{max\text{-}N}$, ●) as a function of nitrogen availability for *S. obliquus* in laboratory culture.

During the outdoor raceway experiment, there were several fertilizer additions. addition, nitrogen was added to the total available nitrogen (Fig. 8). The total available nitrogen was then divided by biomass concentration at each time step. In the early culture, N_A was maintained at a high level; thus there was no significant nitrogen stress, and F_N was maintained at or close 1. With biomass accumulation, N_A decreased rapidly. Lthough nitrogen was added to the culture several times (↑ in Fig. 8), the amount was not enough to prevent growth rate reduction. During most of the experiment, F_N was below 1, indicating that the pond operational practices that were intended to minimize fertilizer cost provided insufficient nitrogen supply. After accounting for nitrogen stress, over-prediction was lowered from 57% to 33% (Fig. 9).

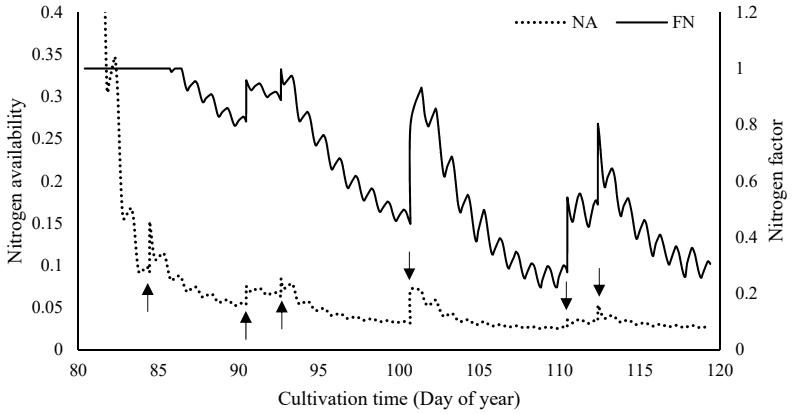

Fig. 8 Nitrogen availability (N_A) and nitrogen factor (F_N) as a function of time during RAFT07 experiment. N_A increases due to nutrient addition (↑).

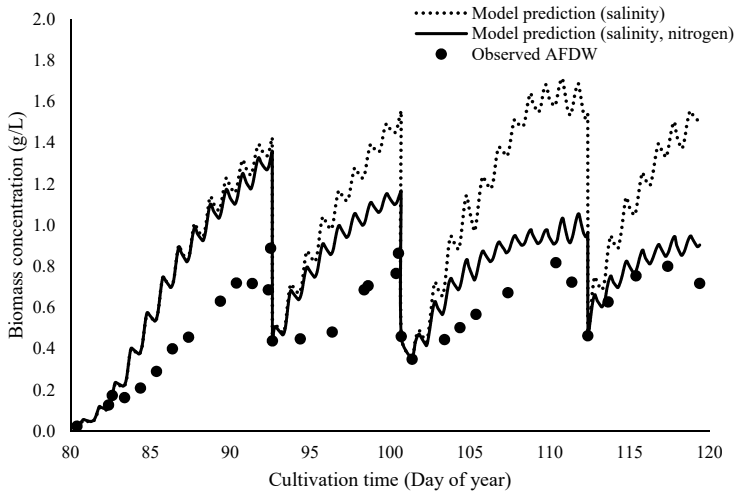

Fig. 9. Measured biomass concentration, prediction of salinity effect adjusted model and prediction of salinity, nitrogen effects adjusted model. $RMSE_3 = 0.30$ and $BF_3 = 1.33$

3.4 Adjustment of the model for shading effect

The measured light intensity ratio (r_{zx}) vs. distance (x) from the baffle at each depth (z) is shown in Figure 10. A linear relationship was found between light ratio and distance from the board at each depth. Light ratios at the edge of shade were close to 30% at all depths. The change of light ratio from 30% in the shade to 100% in the sun takes place within a short distance (< 1cm). Thus, we assumed that the light ratio increased from 30% in the shade to 100% in the sun. The furthest point with the light ratio less than 100% was defined as the edge of shade. Because of the size of sensor, it was impossible to practically measure light intensity at $x = 0$ (next to the board). This value was estimated based on the linear change with distance. The light ratios at the board were within the range of 10% to 14% with average value 12% and standard deviation 1%. The two boundary conditions for r_{zx} were then determined as, $x = 0$, $r_{zx} = 12\%$ and $x = w$, $r_{zx} = 30\%$. Therefore,

$$r_{zx} = 0.18x/w_z + 0.12 \quad (14)$$

Following the procedure described in Theoretical Development, light ratio R_z was calculated.

Case 1, shade at layer z doesn't cover the entire channel ($wz < L$). Equation 6 can be applied directly to find Rz. Substitute Equation 5 into Equation 9 and simplify.

$$R_z = (L\text{-}0.7w_z)/L. \quad (15)$$

Case 2, shade at layer z covers the entire channel ($w_z \geq L$). In this case, there will be no unshaded area; thus, $I_{z\text{-unshaded}} = 0$. The upper limit for the integral (Equation 6) is no longer w_z, but L. Substitute Equation 5 into Equation 9.

$$R_z = \frac{\int_0^L I_{z0} r_{zx} d_x}{I_{z0} L} = 0.09L/w_z + 0.12 \quad (16)$$

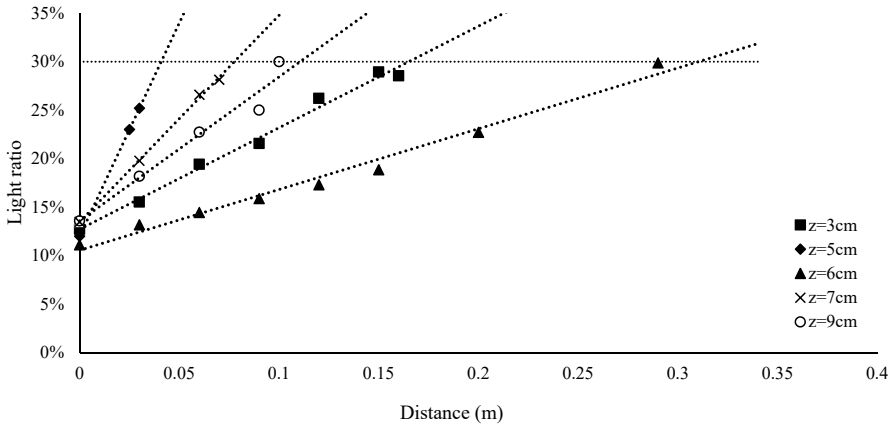

Fig. 10. Light intensity ratio (r_{zx}) as a function of distance from board (x) at different depths (z)

Equation 15 and 16 calculates shading factor R_Z in each layer at depth z. The total shading effect in the culture was expressed as average light ratio, using weighted average of R_Z for the 100 layers. As the experiment approached summer, solar angle increased and led to a higher average light ratio (Fig 11a). Within one day, shade width in early morning and late afternoon is shorter than it in the mid-day within the experimental period; thus, the overall shading effect reaches its maximum at mid-day. Fig. 11b is an example of the overall shading effect variation within DOY100. In general, less than 10% of the light was blocked by shading during this experiment. Incorporation of shading effect lowered model over-prediction from 33% to 22% (Fig. 12). In this experiment, shading exhibited less impact than salinity and nitrogen stress, but in winter or a higher latitude area, its significance would be larger. Cultivation system geometry also has a direct impact on shading effect. For most commercial scale raceways with wide channels and short or sloping berms, shading effect is not significant, but for many smaller scale research raceways, shading may have a significant impact on growth. In these systems, including shading helps to achieve a more accurate and realistic simulation in outdoor raceways.

Commented [高嵩2]: Is this statement clear?

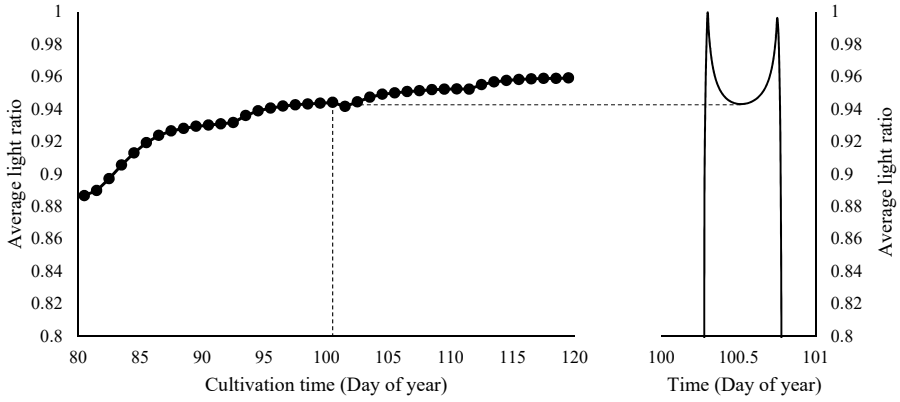

Fig. 11. (a) Average light ratio at mid-day during the experiment. (b) Average light ratio variation within DOY 100. Before sunrise, average light ratio was set to 0. After sunrise, average light ratio increased from 0 to 100% at 7:17 AM, decreased to 94% at 12:33 PM, increased to 100% at 6:00 PM, and decreased to 0 at sunset.

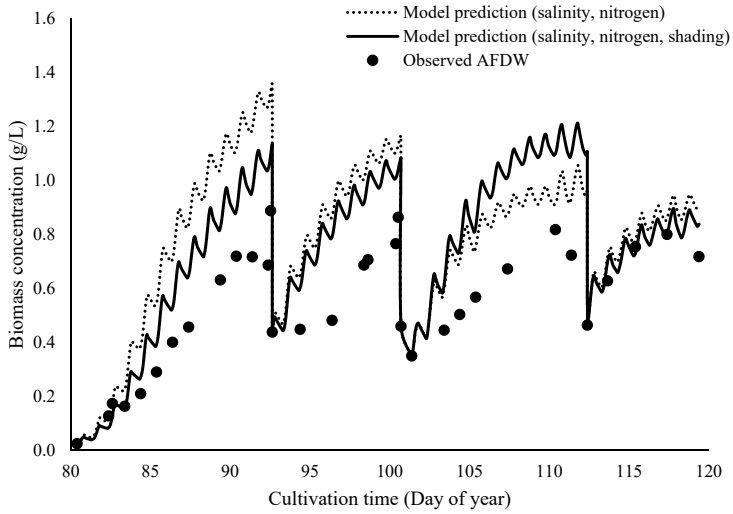

Fig. 12 Measured biomass concentration, prediction of salinity, nitrogen adjusted model and prediction of salinity, nitrogen and shading effect adjusted model. $RMSE_4 = 0.21$, $BF_4 = 1.22$

3.5 Lag phase

In newly inoculated cultures, physiological adaption to the altered conditions usually causes a significantly lower growth rate than in the exponential growth phase (Becker, 1994). During this experiment and many others, we observed that there is a somewhat unpredictable lag phase before exponential growth takes place in each batch. Harvesting may also alter culture conditions and cause reoccurrence of an adaption period. The growth model, $\mu(T, I)$, however, only simulates the exponential growth phase and stationary phase. Thus, the model is limited in capturing growth in lag phase or adaption to new conditions. As mentioned in previous section, the experiment started on DOY 77, followed by a lag phase of three days. The results presented so far have excluded this period. In Fig. 13, the dashed line represents simulated growth without removing lag phase, showing much higher over-prediction. Delaying simulation by 4, 4 and 2 days in batch 1, batch 2 and batch 3 lowered over-prediction to 10%.

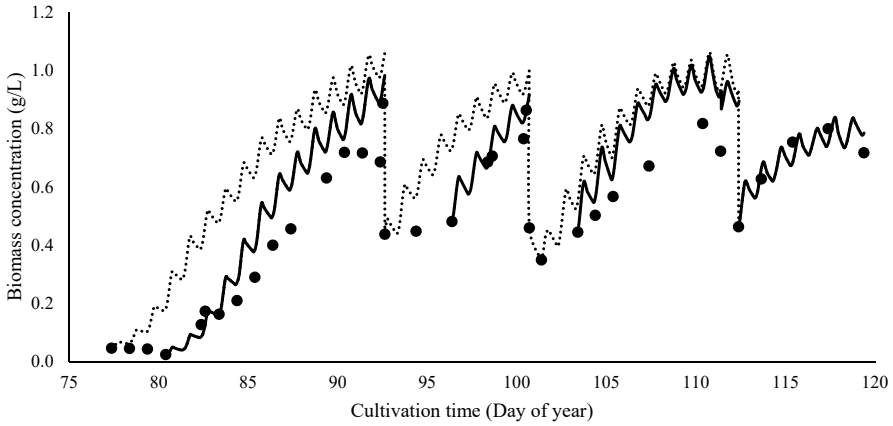

Fig. 13. Comparison of salinity, nitrogen and shading effect modified model with and without lag phase. as well as original model. Delaying simulation by 2 to 4 days resulted in better prediction. $RMSE_5 = 0.16$, $BF_5 = 1.10$

Comparison of the modified model (with all three factors) and RAFT 06 experimental data is showed in Fig. 14. Growth rate in the first batch was lower than expected, but the cause was unknown. Examination of the growth conditions indicated that the reduced growth was not due to weather or contaminants. Both the original model and modified model provided relative good estimation of later growth, this is because that the experiment was conducted with freshwater and sufficient nutrient supply. The influence of modification was not significant due to the absence of salinity or nitrogen stress. The assumptions for the original model were satisfied. Overall, the model provided an accurate estimate of growth rate in two out of three cultural batches (BF = 0.92).

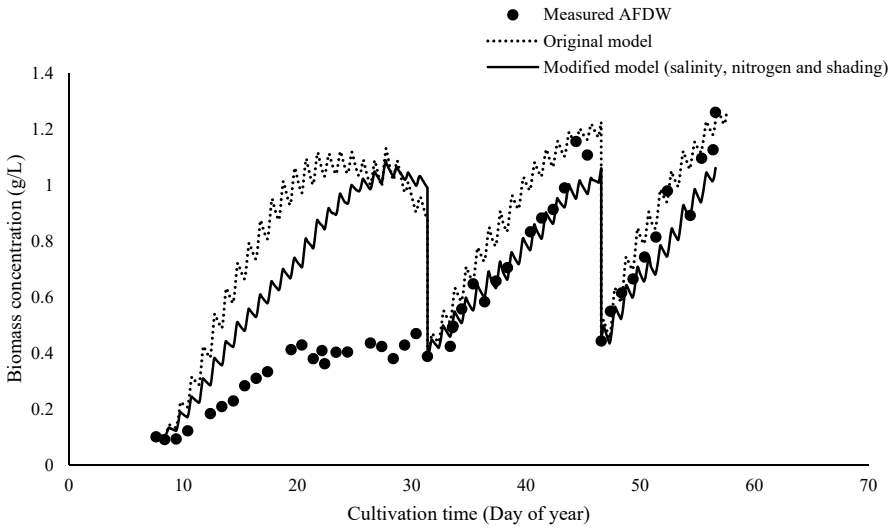

Fig. 14 Comparison of observed growth, original model, and modified model in RAFT06, ARID raceway *Scenedesmus obliquus* experiment. Biomass concentration was reset on DOY 31.

4. Conclusions

In this study, we improved the HABG model (2016) by adding salinity, nitrogen, and shading factors. For the RAFT experiments with high salinity and limited nitrogen supply, the modification greatly improved model prediction. Over-prediction reduced from 90% in the original model to 13% in the modified model for the RAFT07 experiment. (your last statement is not a conclusion.)

Acknowledgement

This study was supported by the U.S. Department of Energy and Regional Algal Feedstock Testbed (RAFT) project, University of Arizona, for which the authors are grateful.

References

Bannister, T.T., 1979. Quantitative description of steady state , algal growth , including adaptation. Limnol. Oceanogr. 24, 76–96.

Baranyi, J., Pin, C., Ross, T., 1999. Validating and comparing predictive models. Int. J. Food Microbiol. 48, 159–166. doi:10.1016/S0168-1605(99)00035-5

Becker, E.W., 1994. Microalgae: Biotechnology and Microbiology. Cambridge University Press, Cambridge, UK.

Converti, A., Casazza, A. a., Ortiz, E.Y., Perego, P., Del Borghi, M., 2009. Effect of temperature and nitrogen concentration on the growth and lipid content of Nannochloropsis oculata and Chlorella vulgaris for biodiesel production. Chem. Eng. Process. 48, 1146–1151. doi:10.1016/j.cep.2009.03.006

Cornet, J.-F., Dussap, C.-G., 2009. A Simple and Reliable Formula for Assessment of Maximum Volumetric Productivities in Photobioreactors. Biotechnol. Prog. 25, 424–435. doi:10.1021/bp.138

Difusa, A., Talukdar, J., Kalita, M.C., Mohanty, K., Goud, V. V., 2015. Effect of light intensity and pH condition on the growth, biomass and lipid content of microalgae Scenedesmus species. Biofuels 6, 37–44. doi:10.1080/17597269.2015.1045274

Droop, M.R., 1968. Vitamin B12 and Marine Ecology. IV. The Kinetics of Uptake, Growth and Inhibition in Monochrysis Lutheri. J. Mar. Biol. Assoc. United Kingdom 48, 689–733.

Edmundson, S.J., Kruk, R., Huesemann, M.H., n.d. Winter Algae Crops: Characterization of Algal Strains with Cold Season Production Potential. Environ. Exp. Bot.

Goldman, J.C., Hole, W., 1979. Outdoor Algal Mass Cultures - II. Photosynthetic Yield Limitations. Water Res. 13, 119–136.

Hsieh, C.H., Wu, W.T., 2009. Cultivation of microalgae for oil production with a cultivation strategy of urea limitation. Bioresour. Technol. 100, 3921–3926. doi:10.1016/j.biortech.2009.03.019

Huesemann, M., Crowe, B., Waller, P., Chavis, A., Hobbs, S., Edmundson, S., Wigmosta, M., 2016. A validated model to predict microalgae growth in outdoor pond cultures subjected to fluctuating light intensities and water temperatures. Algal Res. 13, 195–206. doi:10.1016/j.algal.2015.11.008

James, S.C., Boriah, V., 2010. Modeling Algae Growth in an Open-Channel Raceway. J. Comput. Biol. 17, 895–906. doi:10.1089/cmb.2009.0078

Kaewkannetra, P., Enmak, P., Chiu, T., 2012. The effect of CO2 and salinity on the cultivation of scenedesmus obliquus for biodiesel production. Biotechnol. Bioprocess Eng. 17, 591–597. doi:10.1007/s12257-011-0533-5

López, S., Prieto, M., Dijkstra, J., Dhanoa, M.S., France, J., 2004. Statistical evaluation of mathematical models for microbial growth. Int. J. Food Microbiol. 96, 289–300. doi:10.1016/j.ijfoodmicro.2004.03.026

Mohammed, A.A., Shafea, A.A., 1992. Growth and some metabolic activities of Scenedesmus obliquus cultivated under different NaCl concentrations. Biol. Plant. 34, 423–430.

Packer, A., Li, Y., Andersen, T., Hu, Q., Kuang, Y., Sommerfeld, M., 2011. Growth and neutral lipid synthesis in green microalgae: a mathematical model. Bioresour. Technol. 102, 111–7. doi:10.1016/j.biortech.2010.06.029

Quinn, J., de Winter, L., Bradley, T., 2011. Microalgae bulk growth model with application to industrial scale systems. Bioresour. Technol. 102, 5083–92. doi:10.1016/j.biortech.2011.01.019

Ranga Rao, a, Ravishankar, G. a, Sarada, R., 2012. Cultivation of green alga Botryococcus braunii in raceway, circular ponds under outdoor conditions and its growth, hydrocarbon production. Bioresour. Technol. 123, 528–33. doi:10.1016/j.biortech.2012.07.009

Rao, A.R., Dayananda, C., Sarada, R., Shamala, T.R., Ravishankar, G.A., 2007. Effect of salinity on growth of green alga Botryococcus braunii and its constituents. Bioresour. Technol. 98, 560–564. doi:10.1016/j.biortech.2006.02.007

Rippka, R., Deruelles, J., Waterbury, J.B., Herdman, M., Stanier, R.Y., 1979. Generic Assignments, Strain Histories and Properties of Pure Cultures of Cyanobacteria. J. Gen. Microbiol. 111, 1–61. doi:10.1099/00221287-111-1-1

Rogers, J.N., Rosenberg, J.N., Guzman, B.J., Oh, V.H., Elena, L., Ghassemi, A., Betenbaugh, M.J., Oyler, G.A., Donohue, M.D., 2014. A critical analysis of paddlewheel-driven raceway ponds for algal biofuel production at commercial scales. Algal Res. 4, 76–88. doi:10.1016/j.algal.2013.11.007

Ross, T., 1996. Indices for performance evaluation of predictive models in food microbiology. J. Appl.

Bacteriol. 81, 501–508. doi:10.1111/j.1365-2672.1996.tb03539.x

Sorokin, C., Krauss, R.W., 1958. The effects of light intensity on the growth rates of green algae. Plant Physiol. 33, 109–13. doi:10.2307/4259285

te Giffel, M.C., Zwietering, M.H., 1999. Validation of predictive models describing the growth of Listeria monocytogenes. Int. J. Food Microbiol. 46, 135–49. doi:10.1016/S0168-1605(98)00189-5

Thimijan, R.W., Heins, R.D., 1983. Photometric, radiometric, and quantum light units of measure: a review of procedures for interconversion. HortScience 18, 818–822.

Van Wagenen, J., Holdt, S.L., De Francisci, D., Valverde-Pérez, B., Plósz, B.G., Angelidaki, I., 2014. Microplate-based method for high-throughput screening of microalgae growth potential. Bioresour. Technol. 169, 566–572. doi:10.1016/j.biortech.2014.06.096

Waller, P., Ryan, R., Kacira, M., Li, P., 2012. The algae raceway integrated design for optimal temperature management. Biomass and Bioenergy 46, 702–709. doi:10.1016/j.biombioe.2012.06.025

Wijffels, R.H., Barbosa, M.J., 2010. An outlook on microalgal biofuels. Science 329, 796–799. doi:10.1126/science.1189003

Yoshimura, T., Okada, S., Honda, M., 2013. Culture of the hydrocarbon producing microalga Botryococcus braunii strain Showa: Optimal CO2, salinity, temperature, and irradiance conditions. Bioresour. Technol. 133, 232–239. doi:10.1016/j.biortech.2013.01.095

Yuan, S., Zhou, X., Chen, R., Song, B., 2014. Study on modelling microalgae growth in nitrogen-limited culture system for estimating biomass productivity. Renew. Sustain. Energy Rev. 34, 525–535. doi:10.1016/j.rser.2014.03.032